Anal. Chem. **2005,** *77,* 4013−4019

Glucose Sensing Using Near-Infrared Surface-Enhanced Raman Spectroscopy: Gold Surfaces, 10-Day Stability, and Improved Accuracy

Douglas A. Stuart,† Chanda Ranjit Yonzon,† Xiaoyu Zhang,† Olga Lyandres,‡ Nilam C. Shah,† Matthew R. Glucksberg,‡ Joseph T. Walsh,‡ and Richard P. Van Duyne*,†

Department of Chemistry and Department of Biomedical Engineering, Northwestern University, 2145 Sheridan Road, Evanston, Illinois, 60208-3113

This research presents the achievement of significant milestones toward the development of a minimally invasive, continuously monitoring, glucose-sensing platform based on the optical quantitation of glucose in interstitial fluid. We expand our initial successes in the measurement of glucose by surface-enhanced Raman scattering (SERS), demonstrating substantial improvements not only in the quality and optical properties of the substrate system itself but also in the robustness of the measurement methodology and the amenability of the technique to compact, diode laser-based instrumentation. Herein, we compare the long-term stability of gold to silver film over nanosphere (AuFON, AgFON) substrates functionalized with a partitioning self-assembled monolayer (SAM) using both electrochemical and SERS measurements. AuFONs were found to be stable for a period of at least 11 days. The switch to AuFONs not only provides a more stable surface for SAM formation but also yields better chemometric results, with improved calibration and validation over a range of 0.5−44 mM (10−800 mg/dL). Measured values for glucose concentrations in phosphate-buffered saline (pH ~7.4) based on 160 independent SERS measurements on AuFONs have a root-mean-square error of prediction of 2.7 mM (49.5 mg/dL), with 91% of the values falling within an extended A−B range on an expanded Clarke error grid. Furthermore, AuFONs exhibit surface plasmon resonances at longer wavelengths than similar AgFONs, which make them more efficient for SERS at near-infrared wavelengths, enabling the use of low-power diode lasers in future devices.

The routine electrochemical determination of blood glucose concentrations by diabetics is arguably the single most common analytical measurement made on a given day in the United States. Therefore, analytical methods that can improve on existing technologies by lowering cost, improving accuracy, or increasing ease of use stand to directly benefit the 18 million American diabetics.[1] The accurate measurement of glucose is challenging, particularly in complex biological fluids, which by nature vary greatly in their constituents, not only between individuals but also throughout the day for a particular individual.

Currently, the most successful methods for glucose detection are indirect measurements that rely on the natural affinities of proteins such as glucose oxidase.[2,3] The uncomfortable "finger stick" measurement familiar to diabetics relies on the electrochemical detection of the redox species produced by the enzymatic reduction of glucose by glucose oxidase.[2] Given the success of the enzymatic technique, due primarily to the protein's inherent amenability to biological environments and high affinity for glucose, many research groups have attempted to utilize glucose-sensitive enzymes in novel, nonelectrochemical techniques. For example, Pishko and co-workers used fluorescence resonance energy transfer (FRET) to measure glucose by incorporating fluorescently labeled concanavalin A and dextran in a poly(ethylene glycol) hydrogel matrix.[4] Glucose competitively binds to the concanavalin A, displacing the dextran, thus separating the protein/dextran FRET pair. The increase in the fluorescence of the dextran label was used to track changes in the glucose concentration. Pei and co-workers recently reported on a microcantilever system sensitive to glucose.[5] Glucose oxidase was immobilized onto a microfabricated cantilever surface, which undergoes bending due to surface stress changes upon binding of glucose. The above methods all experience similar limitations because they rely on the same core chemistry—the protein-mediated binding of glucose. Proteins have inherently finite stability, particularly in terms of enzyme turnover lifetime, leading to a need to replenish the protein. Such sensors are also sensitive to interferences, e.g., similar monosaccharides, uric acid, acetaminophen, or dissolved oxygen.[3,6] The binding of enzymes is also known to be temperature and pH dependent, variables frequently beyond experimental control in real-world systems.

* To whom correspondence should be addressed: (e-mail) vanduyne@chem.northwestern.edu.

† Department of Chemistry.

‡ Department of Biomedical Engineering.

(1) *All About Diabetes*; American Diabetes Association, http://www.diabetes.org/about-diabetes.jsp (access date 09−08−2004).
(2) Heller, A. *Annu. Rev. Biomed. Eng.* **1999**, *1*, 153.
(3) Wilson, G. S.; Hu, Y. *Chem. Rev.* **2002**, *100*, 2693.
(4) Russell, R. J.; Pishko, M. V.; Gefrides, C. C.; McShane, M. J.; Cote, G. L. *Anal. Chem.* **1999**, *71*, 3126.
(5) Pei, J. H.; Tian, F.; Thundat, T. *Anal. Chem.* **2004**, *76*, 292.
(6) Turner, A. P. F.; Chen, B. N.; Piletsky, S. A. *Clin. Chem.* **1999**, *45*, 1596.

10.1021/ac0501238 CCC: $30.25
Published on Web 05/24/2005

Others have mimicked the specificity of proteins for carbohydrates by using compounds such as boronic acids,[7,8] molecularly imprinted polymers (MIPs),[9,10] or other nonbiological molecules that bind glucose[11] and undergo a subsequent physically observable change. These chemistries have been featured in numerous indirect detection methods including diffraction spectroscopy,[8,12] fluorescence,[4,7,13−15] and colorimetric UV−visible spectroscopy.[16,17] The aforementioned methods have all been used—to varying degrees of success—for glucose detection. However, both boronic acid and imprinted polymer sensors are generally less sensitive to glucose than to other sugars.[11,13] Many of the boronic acids optimally bind glucose at higher than physiological pH, although progress is being made toward synthesizing boronic acid derivatives that bind glucose at lower pH.[18] MIPs similarly exhibit difficulty with selectivity, due to the structural specificity of the "glucose-shaped" binding cavity.[11] Such indirect methods offer a potentially unlimited number of sensitive detection modalities, including signal multiplication. However, they have many possible sources of error, particularly from competing species. Therefore, it is desirable to be able to directly assess the concentration of glucose in solution.

The direct detection of glucose has been a more challenging analytical problem than the indirect measures detailed above. While glucose can be directly assayed by a variety of laboratory techniques (mass spectrometry, chromatography, etc.),[19,20] the number of methods amenable to clinical or personal use is more limited. The majority of the direct glucose detection techniques are optical because of the reagentless, nondestructive, and rapid nature of spectroscopic analysis. Polarimetry has been used to measure glucose levels based on the rotation of light in aqueous humor.[21,22] Unfortunately, other chemical species in aqueous humor, such as ascorbate and albumin, are also optically rotationally active and can mask the concentration of glucose. Furthermore, the birefringence of the cornea itself complicates such polarimetric measurements. Vibrational spectroscopies enable quantitative, molecularly specific data to be acquired that can readily distinguish analytes based on their unique spectroscopic "fingerprints". Researchers are actively pursuing a variety of infrared and near-infrared (NIR) absorbance[23−30] and Raman spectroscopies for glucose detection.[31−38] Current NIR results are impressive, but the instrumental constraints, i.e., size, cost, and power, are presently prohibitive for portable applications. For example, several groups have recently published results demonstrating both sensitive and accurate glucose measurements using infrared absorbance. Unfortunately, the acquisition of high-quality spectral data can require high powers delivered at the sample and lengthy collection times. Raman spectroscopic methods applied to glucose detection also require high powers and long acquisition times due to the very small Raman scattering cross section of glucose, 5.6×10^{-30} cm^2 molecule^{-1} sr^{-1}, as determined by McCreery and co-workers.[39] This is particularly important when samples consisting of complex mixtures are used because other molecules, such as hemoglobin, may be strong scatterers. If sufficiently high in concentration or scattering cross section, the nontarget molecules' Raman scattering can overwhelm the glucose signal. Detection in less complicated media such as interstitial fluid, tears, or the aqueous humor of the eye could potentially ameliorate the difficulties inherent in interpreting spectra with many confounding analytes,[40] but is complicated by the low level of glucose in these fluids relative to blood and the time differential in glucose concentration between blood and secondary fluid levels.[22,41] The higher signal intensity gained from the surface-enhanced Raman scattering (SERS) phenomenon overcomes the limitations imposed by weak signal strength, enabling the use of lower power and shorter acquisition times.[42] When molecules are brought into proximity to nanoscale roughened metal surfaces, the intensified local electromagnetic field generated by the nanoscale structures is able to enhance the observed Raman scattering by 10^6-10^8, and in exceptional cases as much as 10^{14} times.[43−49] Furthermore, SERS is highly surface selective, such

(7) Karnati, V. V.; Gao, X.; Gao, S.; Yang, W.; Ni, W.; Sankar, S.; Wang, B. *Bioinorg. Med. Chem. Lett.* **2002**, *12*, 3373.
(8) Alexeev, V. L.; Sharma, A. C.; Goponenko, A. V.; Das, S.; Lednev, I. K.; Wilcox, C. S.; Finegold, D. N.; Asher, S. A. *Anal. Chem.* **2003**, *75*, 2316.
(9) Parmpi, P.; Kofinas, P. *Biomaterials* **2004**, *25*, 1969.
(10) Byrne, M. E.; Park, K.; Peppas, N. A. *Adv. Drug Delivery Rev.* **2002**, *54*, 149.
(11) James, T. D.; Shinkai, S. Artificial receptors as chemosensors for carbohydrates. In *Host−Guest Chemistry*; Springer−Verlag: Berlin, 2002; Vol. 218; p 159.
(12) Asher, S. A. A., V. L.; Goponenko, A. V.; Sharma, A. C.; Lednev, I. K.; Wilcox, C. S.; Finegold, D. N. *J. Am. Chem. Soc.* **2003**, *125*, 3332.
(13) Badugu, R.; Lakowicz, J. R.; Geddes, C. D. *Anal. Chem.* **2004**, *76*, 610.
(14) Cao, H. S.; Diaz, D. I.; DiCesare, N.; Lakowicz, J. R.; Heagy, M. D. *Org. Lett.* **2002**, *4*, 1503.
(15) James, T. D.; Shinmori, H.; Shinkai, S. *Chem. Commun.* **1997**, 71.
(16) DiCesare, N.; Lakowicz, J. R. *Org. Lett.* **2001**, *3*, 3891.
(17) Aslan, K.; Zhang, J.; Lakowicz, J. R.; Geddes, C. D. *J. Fluoresc.* **2004**, *14*, 391.
(18) Das, S.; Alexeev, V. L.; Sharma, A. C.; Geib, S. J.; Asher, S. A. *Tetrahedron Lett.* **2003**, *44*, 7719.
(19) Blanco Gomis, D.; Muro Tamayo, J.; Alonso., M. *Anal. Chim. Acta* **2001**, *436*, 173.
(20) Di Gioia, M. L.; Leggio, A.; Le Pera, A.; Liguori, A.; Napoli, A.; Siciliano, C.; Sindona, G. *J. Chromatogr., B* **2004**, *801*, 355.
(21) Cameron, B. D.; Gorde, H. W.; Satheesan, B.; Cote, G. L. *Diabetes Technol. Ther.* **1999**, *1*, 125.
(22) Klonoff, D. C. *Diabetes Care* **1997**, *20*, 433.
(23) Kasemsumran, S.; Du, Y. P.; Murayama, K.; Huehne, M.; Ozaki, Y. *Anal. Chim. Acta* **2004**, *512*, 223.
(24) Jensen, P. S.; Bak, J.; Ladefoged, S.; Andersson-Engels, S. *Spectrosc. Acta, Part A* **2004**, *60*, 899.
(25) Zhang, L.; Small, G. W.; Arnold, M. A. *Anal. Chem.* **2003**, *75*, 5905.
(26) Wabomba, M. J.; Small, G. W.; Arnold, M. A. *Anal. Chim. Acta* **2003**, *490*, 325.
(27) Shen, Y. C.; Davies, A. G.; Linfield, E. H.; Taday, P. F.; Arnone, D. D.; Elsey, T. S. *J. Biol. Phys.* **2003**, *29*, 129.
(28) Maruo, K.; Tsurugi, M.; Tamura, M.; Ozaki, Y. *Appl. Spectrosc.* **2003**, *57*, 1236.
(29) Jensen, P. S.; Bak, J.; Andersson-Engels, S. *Appl. Spectrosc.* **2003**, *57*, 28.
(30) Arnold, M. A. *Abst. Pap. Am. Chem. Soc.* **2002**, *224*, U114.
(31) Bell, A. F.; Barron, L. D.; Hecht, L. *Carbohydr. Res.* **1994**, *257*, 11.
(32) Berger, A. J.; Wang, Y.; Feld, M. S. *Appl. Opt.* **1996**, *35*, 209.
(33) Lambert, J.; Storrie-Lombardi, M.; Borchert, M. *IEEE LEOS Newsl.* **1998**, *12*, 19.
(34) Enejder, A. M. K.; Koo, T. W.; Oh, J.; Hunter, M.; Sasic, S.; Feld, M. S.; Horowitz, G. L. *Opt. Lett.* **2002**, *27*, 2004.
(35) Mrozek, M. F.; Weaver, M. J. *Anal. Chem.* **2002**, *74*, 4069.
(36) Yonzon, C. R.; Haynes, C. L.; Zhang, X. Y.; Walsh, J. T.; Van Duyne, R. P. *Anal. Chem.* **2004**, *76*, 78.
(37) Berger, A. J.; Itzkan, I.; Feld, M. S. *Spectroc. Acta, Part A* **1997**, *53*, 287.
(38) Shafer-Peltier, K. E.; Haynes, C. L.; Glucksberg, M. R.; Van Duyne, R. P. *J. Am. Chem. Soc.* **2003**, *125*, 588.
(39) McCreery, R. L. *Raman Spectroscopy for Chemical Analysis*; John Wiley & Sons: New York, 2000; Vol. 157.
(40) Lambert, J. L.; Morookian, J. M.; Sirk, S. J.; Borchert, M. S. *J. Raman Spectrosc.* **2002**, *33*, 524.
(41) Bantle, J. P.; Thomas, W. *J. Lab. Clin. Med.* **1997**, *130*, 436.
(42) Chang, R. K.; Furtak, T. E. *Surface Enhanced Raman Scattering*; Plenum Press: New York, 1982.
(43) Campion, A.; Kambhampati, P. *Chem. Soc. Rev.* **1998**, *27*, 241.

that the observed enhancements drop ~1 order of magnitude/nm distance between the molecule and the metal surface.[50] Selective substrates can be fabricated that effectively concentrate the target analyte at the SERS active surface, often rendering signal subtraction, particularly of water, unnecessary.[51−58]

We have previously demonstrated that SERS can be used to directly detect glucose on silver surfaces functionalized with alkanethiol monolayers.[36,38] A SAM of *n*-decane-ω-thiol or (1-mercaptoundeca-11-yl)tri(ethylene glycol) partitioned glucose from aqueous buffer into the zone of electromagnetic field enhancement extending from a silver film over nanosphere (AgFON) surface. Due to the low affinity of glucose toward noble metal surfaces, no SERS spectra of glucose could be obtained in the absence of a partitioning layer. Using appropriate multivariate calibration techniques, we could detect glucose over a very wide range of concentrations, both large (0−4500 mg/dL, 0−250 mM) and clinically relevant (0−450 mg/dL, 0−25 mM).[38] The second-generation sensor was robust enough to survive 3 days in solution and could operate effectively in the presence of serum albumin as a blood serum mimic. [36]

The present work demonstrates significant improvements in all aspects of the SERS glucose sensor. Most importantly, this sensor shows higher predictive accuracy than the second-generation sensor and greater stability of the crucial partitioning SAM. We have striven to increase the glucose SERS signal by concentrating the glucose in proximity to the metal by using a glycosylated thiol with a shorter alkane spacer. Spectroscopic and electrochemical measurements indicate that the novel SAM is stable on gold films over nanospheres (AuFONs) for at least 11 days. We attribute the greater temporal stability of the SAM to the switch from silver to gold FON surfaces. The improved surface chemistry is due to the greater strength of the S−Au bond (~420 kJ/mol) relative to the S−Ag bond (217 kJ/mol).[59] We hypothesize that the greater ordering in the SAMs on gold versus silver surfaces is also partially responsible for the observed improvement in glucose measurement. Furthermore, the localized surface plasmon for AuFONs occurs at longer wavelengths than similar AgFONs. AuFONs work well with red and NIR lasers because the optimal SERS enhancements occur when the excitation wavelength is near the plasmon frequency.[49,60] The use of NIR lasers will present several advantages in subsequent device development. NIR diode lasers are relatively compact, inexpensive, and power efficient. Furthermore, switching to NIR wavelengths will reduce not only the interference from biological autofluorescence in future in vivo applications but also the potential for tissue damage due to the low water and tissue absorption of NIR light.[61,62]

EXPERIMENTAL SECTION

Materials. All the chemicals were of reagent grade or better and were used as purchased. Ag and Au wire (99.99%) were purchased for thermal deposition (D. F. Goldsmith, Evanston, IL). Oxygen-free high-conductivity copper (McMaster-Carr, Chicago, IL) was cut into 18-mm-diameter disks for supporting substrates. NH_4OH, H_2O_2, and CH_3CH_2OH (Fisher Scientific, Fairlawn, VA) were used to clean the substrates and as solvents for the SAM. Surfactant-free white carboxyl-substituted latex polystyrene nanosphere suspensions (390 ± 19.5 nm diameter, 4% solid) were obtained from a commercial vendor (Duke Scientific Corp., Palo Alto, CA). Tungsten vapor deposition boats (R. D. Mathis, Long Beach, CA) were used to evaporate the metal. For substrate and solution preparations, ultrapure water (18.2 MΩ cm^{-1}) from Millipore academic system (Millipore, Marlborough, MA) and phosphate-buffered saline (pH ~7.4) (Sigma, St. Louis, MO) were used. 1-Mercaptoocta-8-yltri(ethylene glycol), EG3, was custom synthesized (SensoPath Technologies, Bozeman, MT). Ruthenium hexamine was purchased from Strem (Strem Chemicals, Newburyport, MA).

Substrate Fabrication and Incubation Procedure. The design and fabrication of the SAM-functionalized SERS sensors are shown in Figure 1. Ag- and AuFONs were fabricated on copper substrates, which provide better mechanical stability of the FON than on glass. The copper substrates were cleaned by sonicating in 10:1:1 H_2O/30% H_2O_2/NH_4OH. To form a nanosphere deposition mask, ~12 μL of nanosphere solution was drop-coated onto a clean copper substrate and allowed to dry at room temperature. Then, 200-nm-thick Ag or Au films were deposited onto and through the nanosphere mask using a modified vapor deposition system (Consolidated Vacuum Corp., Rochester, NY) with a base pressure 10^{-7} Torr. The mass thickness and deposition rate (~1 nm/s) of the metal were measured by an Inficon XTM/2 quartz crystal microbalance (Leybold, East Syracuse, NY). The FON substrates were first incubated in 1 mM solutions of the EG3 in ethanol for at least 12 h. Then, the SAM-modified substrates were mounted into a small-volume flow cell. Finally, the substrates were exposed to glucose solutions for at least 5 min, and spectra data were acquired.

UV−Visible Diffuse Reflectance Spectroscopy. Measurements were carried out in a home-built flow cell using an SD2000 spectrometer (Ocean Optics, Dunedin, FL) coupled to a reflectance probe and a model F-O-Lite H halogen lamp (World Precision Instruments, Sarasota, FL). The reflectance probe consists of a tight bundle of 12 read fibers (200 μm) around 1 illumination fiber (400 μm), optimized for the UV−NIR (250−

(44) John T. Krug, I., Geoffrey D. Wang, Steven R. Emory, and Shuming Nie. *J. Am. Chem. Soc.* **1999**, *121*, 9208.
(45) Nie, S.; Emory, S. R. *Science* **1997**, *275*, 1102.
(46) Kneipp, K.; Wang, Y.; Kneipp, H.; Perelman, L. T.; Itzkan, I.; Dasari, R. R.; Feld, M. S. *Phys. Rev. Lett.* **1997**, *78*, 1667.
(47) Otto, A.; Mrozek, I.; Grabhorn, H.; Akemann, W. *J. Phys. Condens. Matter* **1992**, *4*, 1143.
(48) Schatz, G. C.; Van Duyne, R. P. Electromagnetic Mechanism of Surface-Enhanced Spectroscopy. In *Handbook of Vibrational Spectroscopy*; Chalmers, J. M., Griffiths, P. R., Eds.; Wiley: New York, 2002; Vol. 1; pp 759
(49) Haynes, C. L.; Van Duyne, R. P. *J. Phys. Chem. B* **2003**, *107*, 7426.
(50) Kennedy, B. J.; Spaeth, S.; Dickey, M.; Carron, K. T. *J. Phys. Chem. B* **1999**, *103*, 3640.
(51) Deschaines, T. O.; Carron, K. T. *Appl. Spectrosc.* **1997**, *51*, 1355.
(52) Carron, K.; Peitersen, L.; Lewis, M. *Environ. Sci. Technol.* **1992**, *26*, 1950.
(53) Sulk, R.; Chan, C.; Guicheteau, J.; Gomez, C.; Heyns, J. B. B.; Corcoran, R.; Carron, K. *J. Raman Spectrosc.* **1999**, *30*, 853.
(54) Sulk, R. A.; Corcoran, R. C.; Carron, K. T. *Appl. Spectrosc.* **1999**, *53*, 954.
(55) Wachter, E. A.; Storey, J. M. E.; Sharp, S. L.; Carron, K. T.; Jiang, Y. *Appl. Spectrosc.* **1995**, *49*, 193.
(56) Mosier-Boss, P. A.; Boss, R. D.; Lieberman, S. H. *Langmuir* **2000**, *16*, 5441.
(57) Mosier-Boss, P. A.; Lieberman, S. H. *Appl. Spectrosc.* **2003**, *57*, 1129.
(58) Carron, K. T.; Corcoran, R. *Abstr. Pap. Am. Chem. Soc.* **1997**, *214*, 18.
(59) *CRC Handbook of Chemistry and Physics*, 81 ed.; Lide, D. R., Ed.; CRC Press: Boca Raton, FL, 2000; p 2556.
(60) McFarland, A. D., Ph.D. Northwestern University, Evanston, IL, 2004.
(61) Anderson, R. R.; Parrish, J. A. Optical Properties of Human Skin. In *The Science of Photomedicine*; Regan, J. D., Parrish, J. A., Eds.; Plenum Press: New York, 1982; p 147.
(62) Weissleder, R. *Nat. Biotechnol.* **2001**, *19*, 316.

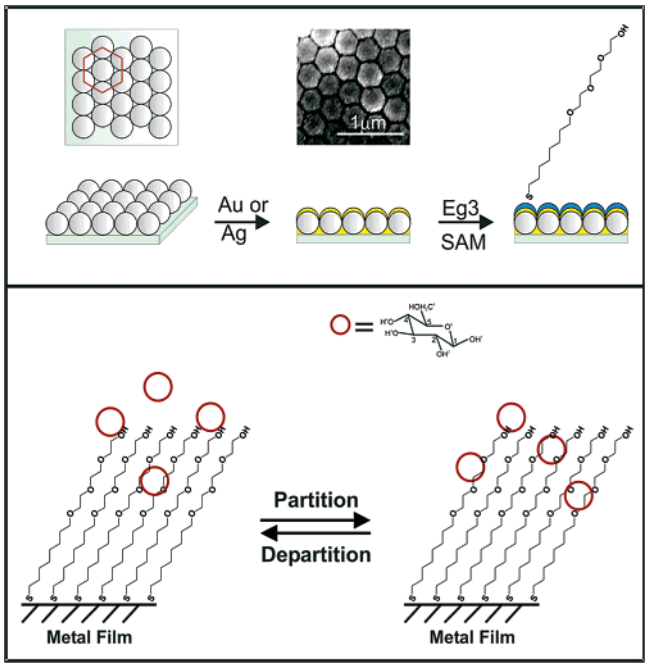

Figure 1. Schematic of sensing surface. Polymer nanospheres are self-assembled onto a supporting substrate, and allowed to form a hexagonal close-packed 2D crystal. Metal (Au or Ag) is then deposited via vacuum thermal deposition over the nanosphere lattice. A SEM micrograph is shown. The Au or Ag FON is then incubated in a solution of EG3, forming a SAM of the EG3. Glucose is able to partition and departition into the monolayer.

2100 nm) in a stainless steel ferrule. All reflectance spectra were collected using a mirrorlike Ag film over copper substrate as a reference.

Electrochemistry. The home-built smooth Ag working electrode was embedded into a glass body using Torr Seal (Varian Vacuum Products, Lexington, MA). Prior to use, surfaces were polished with 0.3- and 0.05-μm alumina, successively (Buehler Ltd., Lake Bluff, IL), and sonicated in MQ water. The Au working electrode, Pt auxiliary electrode, Ag/AgCl reference electrode, and BAS 100B/W electrochemical workstation were acquired commercially (Bioanalytical Systems Inc., West Lafayette, IN). The potential of the Ag/AgCl reference electrodes is −35 mV relative to the saturated calomel electrode.

Surface-Enhanced Raman Scattering Spectroscopy. A Spectra-Physics model Millennia Vs laser was used to excite a Spectra-Physics model 3900 Ti−sapphire laser to produce the 750-nm excitation wavelength (λ_{ex}); the laser spot size on the sample was less than 0.5 mm in diameter. The SERS measurement system includes an interference filter (Edmund Scientific, Barrington, NJ), a holographic notch filter (Kaiser Optical Systems, Ann Arbor, MI), a model VM-505 single-grating monochromator with the entrance slit set at 100 μm (Acton Research Corp., Acton, MA), and a LN_2-cooled CCD detector (Roper Scientific, Trenton, NJ). A collection lens with magnification 5 was used to collect the scattered light. The small-volume flow cell was used to control the external environment of the metal FON surfaces throughout the SERS experiments.

Quantitative Multivariate Analysis. All data processing was performed using MATLAB (MathWorks, Inc., Natick, MA) and PLS_Toolbox (Eigenvector Research, Inc., Manson, WA). Prior to analysis, the spectra were smoothed using a Savitzky−Golay method with a second-order polynomial and window size of 9. Cosmic rays were removed from the spectra using a derivative filter. The slowly varying background, commonly seen in SERS experiments, was removed mathematically by subtracting a fourth-order polynomial. This method minimally affected the SERS peaks while greatly reducing the background level. The SERS spectral intensities were normalized using the 700 ± 10 cm^{-1} peak from the EG3 partition layer spectrum. The 700-cm^{-1} band arises from the S−C bond strech and serves as a convenient reference for SERS of thiol SAMs on metal surfaces.[63] From each spectrum, the absolute peak intensity of the 700-cm^{-1} peak was obtained and the entire spectrum was divided by that value, such that the intensity of the 700-cm^{-1} peak is unity. Then, data analysis was performed using the partial least-squares (PLS) analysis and leave-one-out cross-validation algorithm.

RESULTS AND DISCUSSION

The results presented below detail the achievement of a substantial advance toward the development of a practical, portable, SERS-based glucose measuring device. Our previous work demonstrated the feasibility of using SERS to detect and quantify glucose. Subsequent work addressed the performance of the SERS sensor in terms of short-term stability, reversibility, and selectivity in the presence of interferences. Herein, we report on the development of a substrate that is optimized for SERS using NIR laser excitation with not only enhanced spectral and physical stability but also the capability of superior quantitative measurements.

Optical Properties of Au- and AgFONs. In normal Raman scattering, the signal intensity scales with the inverse fourth power of the excitation wavelength. Thus, the ratio of normal Raman scattering intensities for 750- versus 632.8-nm excitation is 0.51. In contrast, the SERS signal intensity is actually larger when using far-red excitation due the smaller imaginary portion of the complex dielectric constants of Ag and Au. The optical properties of nanoscale noble metal materials, including FONs, are dominated by the surface plasmon.[64] The position and intensity of the surface plasmon is sensitive to the morphology (size and shape) and composition of the material.[65,66] In FONs, the position of the plasmon can be tuned by controlling the size of the spheres used in the underlying nanosphere mask. The surface plasmon is responsible for the intense local electromagnetic fields that give rise to SERS. The maximum SERS enhancements occur when the excitation laser is of slightly shorter wavelength than the surface plasmon, enabling electromagnetic enhancements of both the incoming photons and the scattered, Raman-shifted photons.[49] Therefore, by tuning the physical properties of the FON surface, we are able to tune the surface plasmon to maximize the SERS enhancements. As illustrated in Figure 2, using an AuFON rather than an AgFON enables us to position the plasmon peak nearer the excitation wavelength (λ_{ex}) with greater facility. Although the maximum SERS enhancements on silver surfaces are greater than

(63) Bryant, M. A.; Pemberton, J. E. *J. Am. Chem. Soc.* **1991**, *113*, 8284.
(64) Kreibig, U.; Vollmer, M. *Optical Properties of Metal Clusters*; Springer: New York, 1995.
(65) Haynes, C. L.; Van Duyne, R. P. *Abstr. Pap. Am. Chem. Soc.* **2001**, *222*, U89.
(66) Haynes, C. L.; Van Duyne, R. P. *J. Phys. Chem. B* **2001**, *105*, 5599.

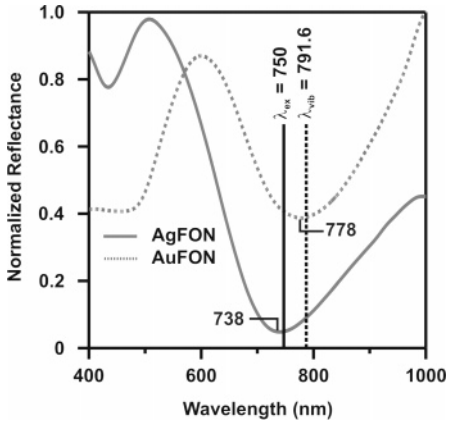

Figure 2. Reflectance spectra from EG3-functionalized Au and AgFONs. The position of the LSPR λ_{min} for the AgFON (738 nm) occurs at shorter wavelengths than that of the AuFON (778 nm). The AuFON is therefore better tuned to the wavelength of the excitation laser used in these experiments (750 nm). The 700-cm^{-1} band of the EG3 SAM occurs at 791.6 nm under 750-nm exitation.

the maximum enhancements on gold surfaces, the efficiency of SERS on silver is highest in the visible region. Thus, gold surfaces become as effective SERS substrates as silver surfaces when λ_{ex} occurs at longer wavelengths. Experimentally, the magnitude of the observed SERS is slightly higher on the gold surfaces than silver, as described below.

SAM Stability. To continuously monitor glucose levels in vivo, a SERS-based sensor must have an implantable substrate that can be optically addressed either directly through the skin or via an optical fiber. Such an implantable glucose sensor must be stable for at least a three-day period. Three days has been chosen as a target milestone because more frequent changing of the implant would be burdensome on the subject, and the implantable insulin pump has a three-day lifetime. Previous work has demonstrated that bare AgFON surfaces display extremely stable SERS activity when challenged with high potentials,[67] and high temperatures in ultrahigh vacuum,[68] and when studied over a three-day period in the presence of saline and interfering analytes such as blood protein mimics.[36] Toward developing a more stable glucose sensor, we have performed an extensive surface study comparing AgFON versus AuFON using cyclic voltammetry (CV) and SERS.

Electrochemical Analysis. It is essential to have a stable, well-packed SAM on the sensor surface since the SAM is essential to partition glucose for SERS detection. Electrochemical measurements of heterogeneous electron transfer were exploited in order to probe the average behavior of the EG3 assemblies on Ag and Au surfaces and the extent of structural defects over the course of 11 days. Ideally, electron transfer through a well-packed monolayer of alkyl chains occurs via a highly nonadiabatic pathway in which the kinetics exhibit an exponential dependence on the separation distance between the electron donor and the electron acceptor.[69] As the extent of structural defects of the monolayer increases, e.g., due to appearance of pinholes and trapped solvent, the current of heterogeneous electron transfer will be strongly increased. Figure 3 shows the electrochemical behavior of ruthenium(III/II) hexamine on EG3-modified Ag and Au electrodes. The complexes were selected because both $Ru(NH_3)_6^{3+}$ and $Ru(NH_3)_6^{2+}$ are substitutionally inert in aqueous media and undergo rapid heterogeneous electron-transfer reactions in a convenient range of potentials.

The initial voltammograms for the $Ru(NH_3)_6^{3+/2+}$ couple at the EG3-covered surfaces are shown as the day 1 samples. After electrochemical examination in 5 mM $Ru(NH_3)_6\,Cl_3$ PBS solution, the EG3-modified electrodes were removed from the cell, thoroughly rinsed with PBS solution, and then reimmersed into the PBS solution before measuring the next cyclic voltammogram. CV of the $Ru(NH_3)_6^{3+/2+}$ couple on clean, unmodified surfaces is also shown in gray lines in Figure 3 for purposes of comparison. At bare Ag and Au electrodes, the shapes of the current−potential curves and ~60-mV separation between the cathodic and anodic peak currents indicate a diffusion-limited or electrochemically reversible one-electron redox process. The voltammograms for the EG3-modified electrodes are remarkably different: the current is much lower, and most of the current comes from the double layer capacitance. For EG3-modified Ag electrodes, the reduction current increases with the immersion time in PBS, owing to an increase in monolayer defects. However, even after 11-day immersion into the PBS solution, the EG3-coated Au electrode shows much lower reduction current in comparison to the EG3-coated Ag electrode.

The percentages of current maximum obtained in voltammetry from PBS-immersed samples vary with time, as shown in Figure 3C. The percentage represents the average of the absolute value of cathodic and anodic peak current divided by the same value calculated from a clean, unmodified surface.[70] As Figure 3C shows, the percentages of the current maximum increase to 20.0% after 10 days for SAM functionalized silver electrodes, while only 2.4% after 11 days for those made with gold. These results agree with the literature[63] and indicate that SAMs are more stable and better ordered on gold than silver surfaces.

SERS Stability. While the electrochemical measurements confirmed that the SAM was adequately blocking the electroactive surface, they did not directly indicate that the FON retained its SERS properties over that time. Therefore, the stability of the EG3-modified metal FON SERS substrates was studied over a period of 10 days in pH 7.4 PBS buffer at room temperature. SERS spectra were captured every 24 h from the same sample (λ_{ex} = 750 nm, t = 60 s) on an AgFON and an AuFON. Figure 4A and B represents the initial EG3 spectra on AgFON and AuFON, respectively. Figure 4C is the peak intensity at 699 cm^{-1} for EG3 on the AgFON, and Figure 4D is the peak intensity at 698 cm^{-1} for EG3 on the AuFON. The EG3 spectral band positions and relative intensities did not vary significantly over the course of 10 days. Although the peak intensities of EG3 on AgFONs and AuFONs were comparable on the first day, peak intensities decreased as time progresses for the AgFON sample. By the fifth day, the peak intensities of the EG3 on the AgFON diminished to the point where no data could be acquired. The peak intensities of the EG3 on the AuFON, however, remained constant over the period of 10 days. These spectral data not only indicate that the

(67) Zhang, X.; Yonzon, C. R.; Van Duyne, R. P. *Proc. SPIE-Int. Soc. Opt. Eng.* **2003**, *5221*, 82.
(68) Litorja, M.; Haynes, C. L.; Haes, A. J.; Jensen, T. R.; Van Duyne, R. P. *J. Phys. Chem. B* **2001**, *105*, 6907.
(69) Li, T. T. T.; Liu, H. Y.; Weaver, M. J. *J. Am. Chem. Soc.* **1984**, *106*, 1233.
(70) Flynn, N. T.; Tran, T. N. T.; Cima, M. J.; Langer, R. *Langmuir* **2003**, *19*, 10909.

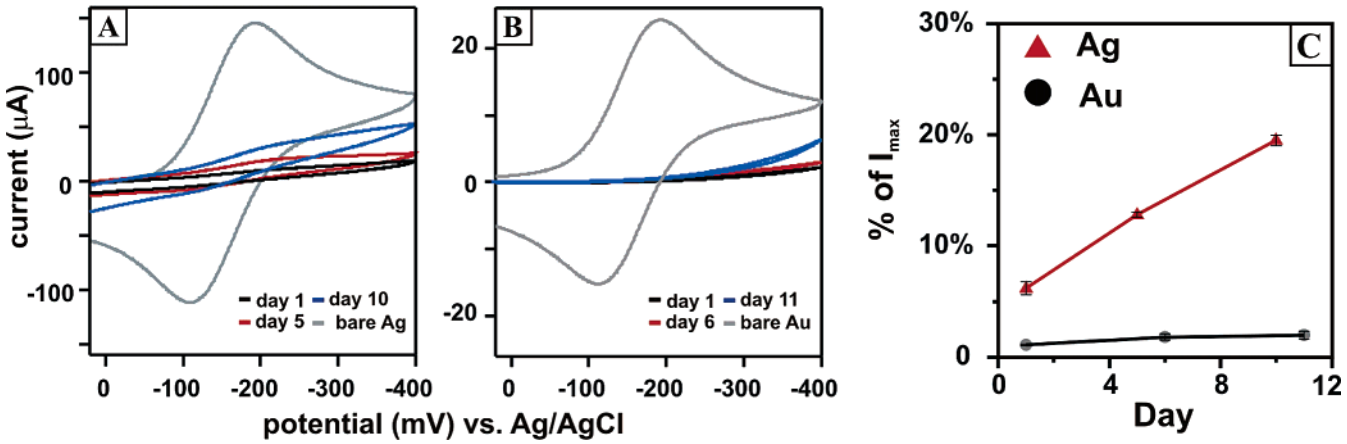

Figure 3. Electrochemical determination of monolayer stability. Both Ag (A) and Au (B) electrodes were functionalized with a SAM and immersed in a solution of 1 mM $Ru(NH_3)_6$ Cl_3 in PBS buffer. Cyclic voltammograms were taken of the electrodes daily for 10 days, with a scan rate of 200 mV/s. Shown are representative voltammograms for days 1 (black), 5 (red), and 10 (blue) on the silver electrode, and days 1 (black), 6 (red), and 11 (blue) on the gold electrode, as well as a reference voltammogram (gray) from a bare (control) electrode (both Au and Ag electrodes). Desorption of the protective monolayer permits direct access to the electrode surface by the electroactive species and was observed as an increase in the total current over time. (C) shows the percentages of current maximum vary with time.

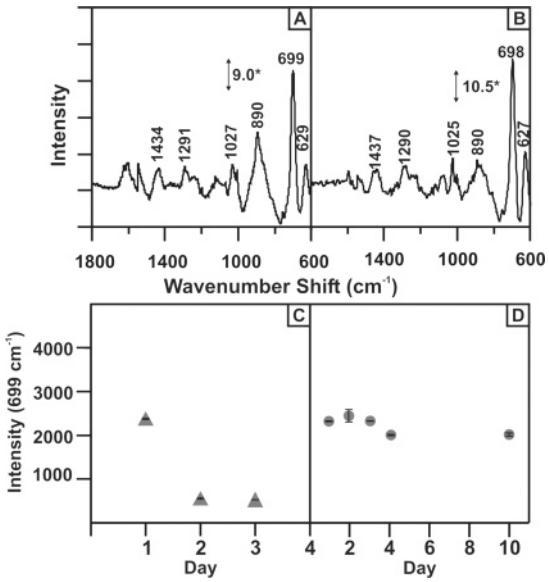

Figure 4. Comparative SERS spectra of EG3 on (A) AgFON and (B) AuFON surfaces. FONs were prepared by coating 390-nm nanospheres with 200 nm of metal. (C) and (D) show the time course of the intensity to the ~699-cm^{-1} peak. Signal intensities from the AuFON remained stable for a period of 10 days. The AgFONs rapidly lost signal, and no spectra were observed by day 4. For all cases, λ_{ex} = 750 nm, 7−8 mW power, and 60-s acquisition.

AuFON surface remains SERS active but also confirm that the SAM is intact and well ordered.

Quantitative Detection. A PLS calibration model was built using 160 independent spectral measurements on sensors exposed to known concentrations of glucose. Data were collected by immersing prepared substrates in glucose solutions and acquiring SERS spectra (λ_{ex} = 750 nm, 10-s integration × 12 averages). Spectra from two locations on the substrate were acquired for each concentration. Several different substrates were used to build the training set, and each of those substrates was exposed to glucose concentrations spanning the experimental concentration range. Based on the calibration, 95% of the data is represented by nine latent variables.

The number of latent variables can be interpreted as the inherent dimensionality of the system, in other words, the number of variables present including the concentration of the analyte of interest. These variables can include, and are not limited to, the temperature and humidity conditions in the laboratory on the day of the experiment, the focusing of the optical elements, the enhancement of the sensing surface at different locations, and the laser power and mode fluctuations, as well as noise in the data. Although using too many latent variables can cause over-modeling of the data, including all of the above-mentioned variation in the experimental design is necessary to build a robust calibration model.[71] For example, the training set needs to be able to accurately predict glucose concentrations at more than one temperature to account for thermal fluctuations in vivo and to still function if subject movement alters the position of the optical focus.

The use of nine latent variables resulted in a model with a root-mean-square error of calibration (RMSEC) of 49.5 mg/dL (2.7 mM). The RMSEC describes the accuracy of the model itself. Our previous work modeled the response for a single sensor surface optically addressed at a single spot. This approach lead to a lower RMSEC, i.e., a precise model, but predictions based on models generated in this manner performed poorly when applied to data collected from either a different focal point or another substrate. Because real-world applications of the sensor will include a number of independent and uncontrolled variables, a versatile mathematical model is needed, and it is reasonable that the dimensionality of the system can be as high as 9. Including a large number of samples in the calibration set helps generate a robust mathematical model by including data that may be affected by the uncontrolled variables. The 160 data points were collected on several unique substrates, and measurements were made on at least two spots on each surface to account for possible differences in the SERS signals arising from variation in the AuFON/SAM microenvironment. Furthermore, the data for the calibration were collected at different times of the day, over a

(71) Beebe, K. R.; Pell, R. J.; Seasholtz, M. B. *Chemometrics: A Practical Guide*; Wiley-Interscience: New York, 1998.

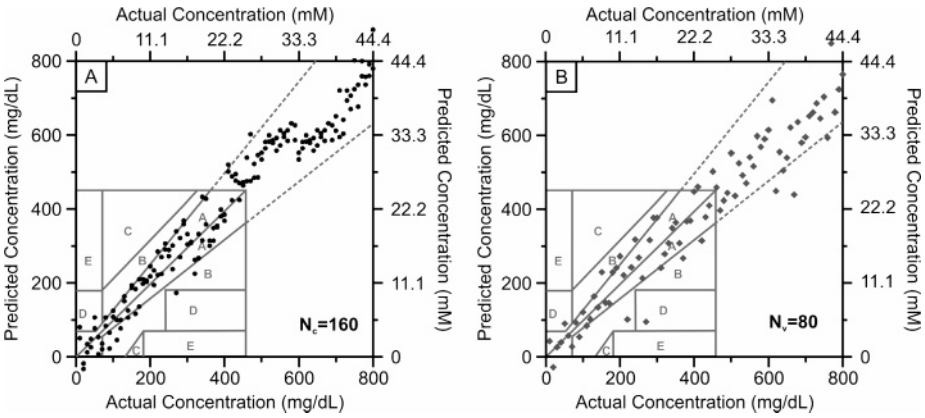

Figure 5. Calibration and prediction/validation plots using multiple substrates. PLS calibration plots were constructed using 160 data points taken over a range of concentrations (10−800 mg/dL) on a number of separately prepared AgFON substrates (5). Each substrate was interrogated at three different locations. Nine latent variables were used to generate the mathematical model, which had an RMSEC of 49.5 mg/dL. The central line represents the ideal prediction axis, not a best-fit curve. An independent validation set was used to test the predictive capability of the mathematical model. Predictions fall primarily within the extended A or B range of the Clarke error grid, with an RMSEP of 69.9 mg/dL.

period of several days. This helps account for random fluctuations in the data and minimizes the residuals and errors in the data analysis. By increasing the number of data samples, we can decrease the RMSEC as well as improve the quantitative prediction of glucose concentration.

A low RMSEC is necessary for, but does not in itself ensure, accurate prediction of concentrations based on measurements from samples outside the training set. Therefore, a separate set of spectra consisting of 80 independent data points was used to validate the model. Validation tests the ability of the model to predict the concentration of samples not used in the calibration, and more precisely reflects the accuracy of the sensor. The RMSEP was calculated to be 69.87 mg/dL (3.88 mM).

In Figure 5, the calibration and prediction data points are plotted against the Clarke error grid, a standard metric for the performance of glucose sensors, to evaluate the predictive capacity of the model.[72] The calibration and prediction shown in Figure 5 are constructed for a range higher than the clinically relevant range (0−450 mg/dL, 0−25 mM) of the Clarke error grid because patients can have elevated blood glucose levels as high as 650−800 mg/dL during initial diagnosis of diabetes. Extending the A lines of the Clarke error grid over the entire range, 94% of the data points in the calibration plot and 91% of data points in the prediction plot fall within the acceptable region. These results indicate that the AuFON sensor is capable of making acceptably accurate concentration measurements even when challenged with a diverse sample population.

CONCLUSIONS

This work details our improvements in detecting and measuring glucose using SERS. Most notably, the sensor system is now able to perform more accurately over a wide range of glucose concentrations, over a long period of time, and on multiple substrates. Validation of the PLS model with 80 independent measurements yields an RMSEP of 2.7 mM (49.5 mg/dL), with 91% of the values falling within an extended A−B range on an expanded Clarke error grid. These analytical figures of merit compare favorably with existing detection methods, which have instrument-dependent coefficients of variation of 0.96−26.9% (0.096−2.69 mM, 1.75−49 mg/dL at 10 mM).[73,74] The partition layer was improved by using 1-mercaptoocta-8-yltri(ethylene glycol), which has a shorter alkyl chain than the SAMs used previously. This shorter spacer is sufficiently alkane in nature to form ordered SAMs on the surface but is shorter thereby increasing the electromagnetic enhancement of the partitioned glucose. Additionally, the underlying SERS substrate transitioned from an AgFON to an AuFON. We have experimentally determined that the SAM is more stable on the gold surface by both cyclic voltammetry and SERS spectroscopy. We have also demonstrated that there are spectroscopic advantages to using AuFONs. The optimal laser wavelengths for SERS can be extended into the red and NIR because the fundamental plasmon wavelength for gold occurs at longer wavelength than silver. Red and NIR wavelengths will reduce background from biological autofluorescence and help prevent signal loss due to tissue and water absorption. Further experiments will test the capability of the sensor for interfacing with compact instrumentation, including fiber delivery and collection optics. In the near term, we will apply this sensor to the measurement of glucose levels in interstitial fluid in rodents.

ACKNOWLEDGMENT

The authors thank Erin M. Hicks for the SEM image used in Figure 1. This work was supported by the Institute for Bioengineering and Nanoscience in Advanced Medicine at Northwestern University, the National Institutes of Health (EY13002 and EY13015), the National Science Foundation (EEC-0118025 and DMR-0076097), and the Air Force Office of Scientific Research MURI program (F49620-02-1-0381).

(72) Clarke, W. L.; Cox, D.; Gonder-Frederick, L. A.; Carter, W.; Pohl, S. L. *Diabetes Care* **1987**, *10*, 622.
(73) Solnica, B.; Naskalski, J. W.; Soeradzki, J. *Clin. Chim. Acta* **2003**, *331*, 29.
(74) Johnson, R. N.; Baker, J. R. *Clinica Chim. Acta* **2001**, *307*, 61.

Received for review January 21, 2005. Accepted April 20, 2005.

AC0501238